ResearchGate

See discussions, stats, and author profiles for this publication at: https://www.researchgate.net/publication/284166910

Synthesis and characterization of polyurethane

DATASET · NOVEMBER 2015

READS

3

Available from: Manish Jain
Retrieved on: 16 January 2016

Published on 27 October 2015. Downloaded by Indian Institute of Technology New Delhi on 19/11/2015 06:28:05.

RSC Advances

PAPER

View Article Online
View Journal | View Issue

Cite this: *RSC Adv.*, 2015, **5**, 95994

Synthesis and characterization of polyurethane/poly(vinylpyridine) composite membranes for desulfurization of gasoline

Mahmood Roostaiy Ghalehnooiy,[ab] Azam Marjani*[b] and Mehdi Ghadiri[c]

Received 15th July 2015
Accepted 27th October 2015

DOI: 10.1039/c5ra13951a

www.rsc.org/advances

Polyurethane/poly(vinylpyridine) (PU/PVP) composite membranes for desulfurizing gasoline were prepared. The membranes were characterized by scanning electron microscopy to confirm the fine dispersion of PVP in PU, and a swelling test was conducted to determine the suitability of composite membranes for desulfurizing gasoline. The hydrophilicity of the membranes was analyzed by measuring the contact angle. The hydrophilicity of mixed matrix membranes was much higher than the pure PU membranes. The performance of the membranes was evaluated in pervaporation desulfurization of gasoline under different operating conditions. The effect on the pervaporation performance of the composite membranes of operational parameters, including feed flow rate, sulfur concentration in the feed stream, and feed temperature, were studied. The permeation flux increased with the feed flow rate and operating temperature, whereas it remained almost constant as the sulfur content in the feed increased. However, the sulfur enrichment factor decreased with increasing sulfur content in the feed stream. In addition, a mathematical model was developed to simulate the pervaporation system. The model was based on solving the continuity equation for sulfur in the feed side and membrane.

1 Introduction

There are various types of sulfur compounds in gasoline such as sulfides, thiols, and mercaptans. These sulfur compounds are converted into sulfur dioxide (SO_2) during gasoline combustion in automobile engines. In addition, most refineries process high-sulfur crude oil because of the low availability of lighter, low-sulfur crude. Environmental regulations that restrict sulfur emissions are continually being lowered; therefore, technical development for deep gasoline desulfurization to prevent the adverse effects of sulfur compounds in fuels is urgently needed, and it is attracting increasing attention.[1–4]

A number of methods have been suggested to decrease the sulfur compound content in gasoline; however, none of them have proved to be useful and efficient on an industrial scale. Hydro-treating the feed is an important process for reducing the sulfur level in gasoline to an appropriate level. However, installing hydro-treating capacity requires considerable capital expense and increases operating costs.[5–7]

Most industrial-scale separation processes are based on energy-intensive approaches such as evaporation, distillation and crystallization. These processes are not sustainable as the worldwide energy crisis deepens. Membrane separation systems have attracted much attention as an alternative to traditional separation systems. Membrane separation processes have benefits, including high separation efficiency, no waste stream, low energy and operating expenses, and suitability for heat-sensitive chemicals, that make them attractive for separating liquid and gas mixtures.[8–10]

Gasoline can be desulfurized by membrane separation technology. Various membrane technologies are used for the separation and purification of liquids by microfiltration, ultrafiltration, reverse osmosis, electrodialysis, and pervaporation. Pervaporation has attracted much attention for separating liquid mixtures owing to its unique advantages. Pervaporation is a low-energy process for desulfurizing gasoline, and creating the vacuum required by the process consumes the majority of the energy.[11–19]

Liquid mixtures are separated into their constituents by pervaporation by using a dense membrane. The transport of species through the membrane occurs because of differences in the chemical potential of components across the membrane. The membrane can be polymeric or ceramic depending on the requirements of the process. The governing separation mechanism in pervaporation is a solution-diffusion mechanism.[13,20,21] In principle, the transport of molecules through the membrane involves three steps: selective sorption of molecules from the feed into the dense membrane; diffusion of molecules through the membrane matrix; and desorption of the molecules

[a]*Islamic Azad University, Farahan Branch, Department of Chemical Engineering, Farahan, Iran*

[b]*Department of Chemistry, Arak Branch, Islamic Azad University, Arak, Iran. E-mail: a-marjani@iau-arak.ac.ir; Fax: +98 861 4132459; Tel: +98 861 4132451*

[c]*Young Researchers and Elite Club, South Tehran Branch, Islamic Azad University, Tehran, Iran*

This journal is © The Royal Society of Chemistry 2015

Published on 27 October 2015. Downloaded by Indian Institute of Technology New Delhi on 19/11/2015 06:28:05.

into the vapor phase on the permeate side.[22,23] Therefore, the transport rate of molecules through the membrane is a function of the solubility and diffusivity because the desorption step is fast owing to the efficient vacuum downstream. Industrial applications of pervaporation technology include removing organic components from aqueous waste, dehydrating solvents, and separating organic/organic mixtures.[24,25]

Polymers, such as polyurethane (PU), polyimide, polydimethylsiloxane, polyethylene glycol, polyphosphazene, polyvinylidene fluoride, polyhedral oligomeric silsesquioxane, and polysulfone, have been used as membrane materials for desulfurizing gasoline.[21,26,27] The performance of membranes has been improved by blending the membrane materials with various filler particles or other polymers, by optimizing the cross linking of polymeric resins or by functionalizing the membrane.[28–30] To our knowledge, pervaporation has not been used for desulfurizing gasoline with PVP/PU composite membranes. In this work, we synthesize and investigate PVP/PU composite membranes for desulfurizing gasoline in a pervaporation system.

The membranes were characterized by scanning electron microscopy and a swelling test. For a refinery naphtha feed stream, the pervaporation and desulfurization performance of the blend membranes under different conditions was investigated. Our results provide useful insights for developing membrane desulfurization technology. Furthermore, a mathematical model is developed to simulate the pervaporation system. The model is based on solving conservation equations for sulfur in the membrane module.

2 Experimental

2.1 Materials

PU and poly(vinylpyridine) (PVP) used to prepare the membranes were purchased from Sigma Aldrich. PU is used in many industrial applications because it shows a wide variety of mechanical properties, from rubber to plastic, and is resistant to different solutions. The refinery naphtha feed was obtained from Imam Khomeini Refinery (Shazand, Iran). Other chemicals were analytical grade reagents and were used as received without further purification.

2.2 Membrane preparation

PU was dissolved in *n*-heptane to form a homogenous solution at room temperature. PVP was added to the stirred solution. To disperse the polymer particles, the suspension was sonicated for 5 min. After filtration and degassing, the solution was cast on a glass plate. The cast film was dried in air, and then in an oven to evaporate the residual solvent. The dried membranes were separated from the glass surface at room temperature and a homogeneous membrane was obtained. The membranes were high quality and were not damaged during the separation. The membranes had high resistance to gasoline. The structure of the membranes was unchanged after they were placed in gasoline for a week.

2.3 Membrane characterization

2.3.1 Scanning electron microscopy (SEM). Scanning electron micrographs of composite membranes were obtained on a scanning electron microscope (SEM; XL-30M, Philips). All specimens were coated with a thin layer of gold prior to analysis to prevent charging.

2.3.2 Contact angle measurement. The hydrophilicity of the pure and mixed matrix membranes was evaluated by measuring the contact angle formed between the membrane surface and a deionized water drop (5 μL). The contact angle was measured at room temperature by using an optical contact angle goniometer (OCA20, Dataphysics Instruments), which uses the static sessile drop method for measuring the contact angle. The contact angle was measured at two random locations for each sample and the average was reported.

2.4 Pervaporation experiments

The performance of the composite membranes for desulfurizing gasoline was assessed with the experimental pervaporation setup shown in Fig. 1. The effect of the feed concentration and temperature on the mass flux and enrichment factor of sulfur was investigated. Feed solutions at different concentrations ranging from 220–800 ppm were prepared and fed to the membrane module at a constant flow rate. The temperature of the feed stream was adjusted between 300 and 360 K with a constant-temperature heat bath. Pervaporation experiments were conducted in cross-flow mode. The composite membrane was placed in the module with an effective area of 13.852 cm^2. A rubber O-ring provided a pressure seal between the module and the blend membrane. Pressure at the permeate side was maintained at 0.3 bar by an oil-sealed vacuum pump (JB, USA). Permeate vapors were condensed and collected in a cold trap (glass vessel) in a liquid nitrogen reservoir. The permeate samples collected in the glass vessel were weighed, and then analyzed by gas chromatography. Total permeation flux (J) was determined with eqn (1).

$$J = \frac{m}{At} \tag{1}$$

Here, m (kg) is the total mass of the permeate collected through effective composite membrane area A (m^2) during time interval t (h). To investigate the reproducibility of the experimental results, all experiments were performed in duplicate.

The enrichment factor is a qualitative criterion for evaluating membrane separation performance. It is written as

$$E = \frac{C_{s,p}}{C_{s,f}} \tag{2}$$

where $C_{s,f}$ (ppm) and $C_{s,p}$ (ppm) are total sulfur content in the feed and permeate streams.

2.5 Mathematical modeling

To predict the separation performance of membranes, a 2D mathematical model was developed in this study. The model is based on solving conservation equations for sulfur in the feed and membrane. This model has been used previously to

Published on 27 October 2015. Downloaded by Indian Institute of Technology New Delhi on 19/11/2015 06:28:05.

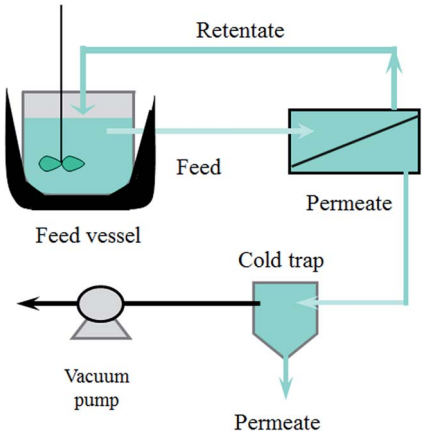

Fig. 1 Experimental setup for pervaporation desulfurization of gasoline.

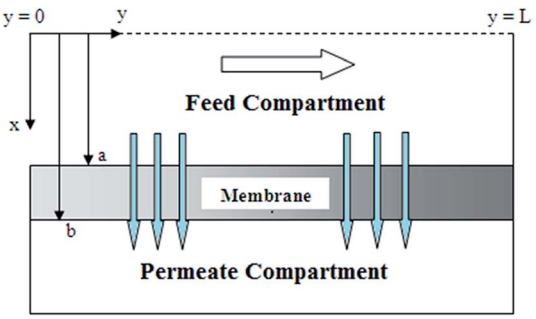

Fig. 2 Model domain used in the simulation.

simulate membrane processes.[31–34] Fig. 2 shows the domain used in the modeling of system.

The feed solution containing sulfur and gasoline is passed to the feed side, the sulfur gathers against the membrane because of the concentration difference, and then diffuses through the dense membrane. Finally, the sulfur desorbs to the permeate side. Thus, the model domain is divided into three sub-domains: feed, membrane, and permeate.

The main equation that describes the transfer of sulfur from gasoline to the permeate side is a continuity equation. This equation is derived from the mass balance of sulfur within an element. The differential form of the continuity equation for sulfur is given as[35]

$$\frac{\partial C_s}{\partial t} + \nabla\cdot(-D_s\nabla C_s + C_s V) = R_s \quad (3)$$

where C_s, D_s, V, and R_s denote sulfur concentration (mol m^{-3}), sulfur diffusivity (m^2 s^{-1}), velocity vector (m s^{-1}), and chemical reaction (mol m^{-3} s^{-1}), respectively. Note that chemical reactions are not considered in the simulation.

Eqn (3) is used for the feed and membrane compartments. To solve eqn (3) for the feed side, the velocity distribution is required. The velocity distribution for the feed side can be calculated *via* solving the Navier–Stokes equations, which may be written as[35–37]

$$-\nabla\cdot\eta(\nabla V_y + (\nabla V_y)^T) + \rho(V_y\cdot\nabla)V_y + \nabla p = F,\ \nabla V_y = 0 \quad (4)$$

where η is the dynamic viscosity (kg m^{-1} s^{-1}), V_y is the velocity vector in the y direction (m s^{-1}), ρ is the fluid density (kg m^{-3}), p is the pressure (Pa), and F is a body force term (N). Eqn (4) is for the steady state operation. Boundary conditions for equations can be categorized according to their domains, which are shown in Table 1.

The model equations with the boundary conditions were solved numerically *via* COMSOL Multiphysics software. A system with the specifications of RAM 4.00 GB (2.98 GB usable) and Intel Core i5CPU M 480@2.67 GHz and a 64 bit operating system was used to solve the model equations. The accuracy of the numerical procedure has been confirmed in previous publications.[31,36,38–45]

3 Results and discussion

3.1 SEM and contact angle characterization

The membranes were characterized by scanning electron microscopy (SEM) to observe the dispersion of PVP in the PU matrix. Fig. 3 shows the SEM images of the membranes with various PVP loadings from a PVP/PU ratio of 0 to 1. No porous structure is visible on the surface of the dense PU membrane in Fig. 3a. Increasing the PVP loading increases the particle distribution in the PU polymer matrix, which reduces the separation performance of the membranes. Increasing the PVP content would result in agglomeration of PVP in the polymer matrix, which is undesirable in the synthesis of high-quality membranes. Increasing the PVP content increases permeation, although it decreases the separation factor drastically.

Table 1 Boundary conditions for momentum and mass transfer equations

Position	Feed side (mass)	Feed side (momentum)	Membrane (mass)
$y = 0$	$C_{\text{s-feed}} = C_0$	$V_y = V_0$	$\frac{\partial C_{\text{s-membrane}}}{\partial y} = 0$
$y = L$	$\frac{\partial C_{\text{s-feed}}}{\partial y} = 0$	$V_y = 0$	$\frac{\partial C_{\text{s-membrane}}}{\partial y} = 0$
$x = 0$	Convective flux	$p = p_{\text{atm}}$	—
$x = a$	$C_{\text{s-feed}} = C_{\text{s-membrane}}/m$	$V_y = 0$	$C_{\text{s-membrane}} = C_{\text{s-feed}} \times m$
$x = b$	—	—	$C_{\text{s-membrane}} = P/RT$

This journal is © The Royal Society of Chemistry 2015

Published on 27 October 2015. Downloaded by Indian Institute of Technology New Delhi on 19/11/2015 06:28:05.

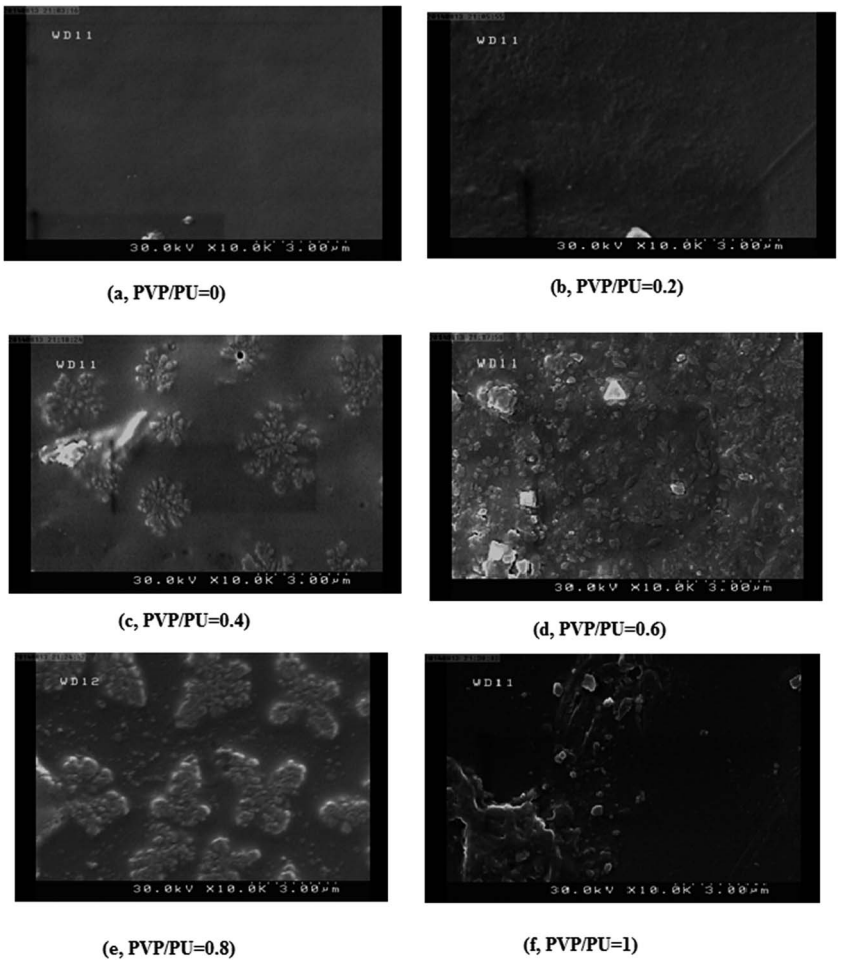

Fig. 3 SEM images of the composite membranes at different PVP loadings. (a) Pure PU; PVP/PU = (b) 0.2; (c) 0.4; (d) 0.6; (e) 0.8; (f) and 1.

Moreover, at high PVP loadings, agglomerates 3 μm in size were observed.

Fig. 4 shows the contact angles for pure PU and mixed matrix membranes containing PVP. Compared with the pure PU membrane, the contact angle of mixed matrix membranes decreased substantially, indicating that the mixed matrix membranes were more hydrophilic. Generally, materials with a lower water contact angle are more hydrophilic.[46] The surface tensions of pure PU and mixed matrix membranes are shown in Table 2. Increasing the content of PVP in the mixed matrix membranes decreased the surface tension. Thus, the hydrophilicity of mixed matrix membrane increased with an increase in PVP content.

Fig. 4 Contact angles for 0%, 40%, and 80% PVP.

Published on 27 October 2015. Downloaded by Indian Institute of Technology New Delhi on 19/11/2015 06:28:05.

Table 2 Surface tension of 0%, 40%, and 80% PVP

Sample	Surface tension	Unit
0% PVP	77.1	(mN m^{-1})
40% PVP	55.6	(mN m^{-1})
80% PVP	51.1	(mN m^{-1})

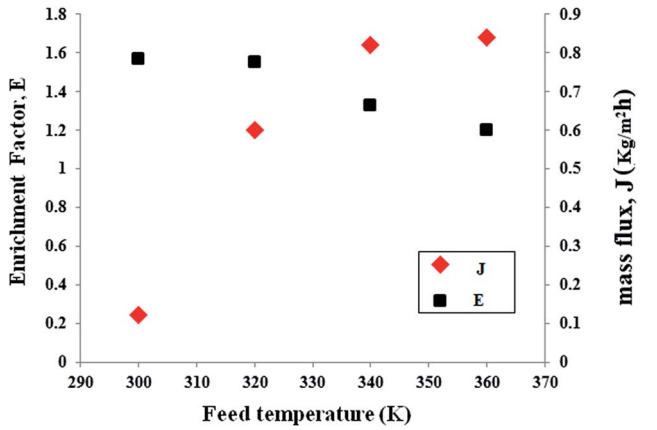

Fig. 5 Effect of temperature on mass flux and enrichment factor. The sulfur concentration in the feed is 200 ppm (PVP/PU = 0.2).

3.2 Effect of feed temperature

The enrichment factor and mass transfer flux as function of feed temperature are shown in Fig. 5. Temperatures from 300 to 360 K were considered to evaluate the effect of feed temperature. The permeation flux was increased by increasing the feed temperature because the transport mechanism in pervaporation systems with dense membranes is the solution-diffusion mechanism.[47,48] Increasing the temperature would increase the solubility and diffusivity of sulfur in the composite membrane (PVP/PU = 0.2). In addition, the free volume in the polymer structure increases with increasing temperature, which makes the transfer of molecules from one side to the other easy. Consequently, increasing flux increases the amount of non-sulfur hydrocarbon molecules that penetrate to the permeate side, reducing the enrichment factor (Fig. 5). The maximum enrichment factor is obtained at a feed temperature of 300 K.

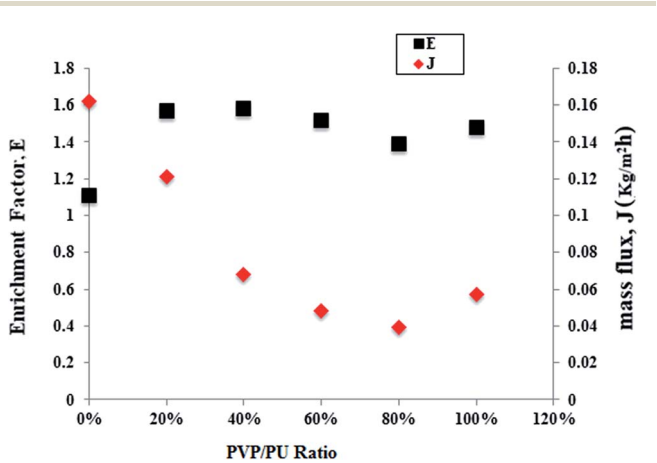

Fig. 6 Effect of the amount of PVP on pervaporation performance.

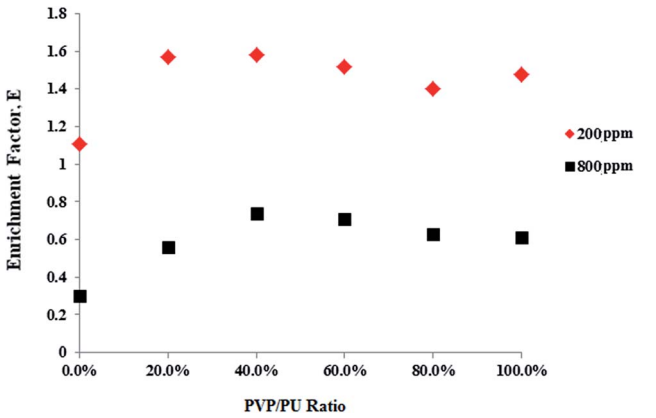

Fig. 7 Effect of sulfur content on the enrichment factor. $T = 25$ °C.

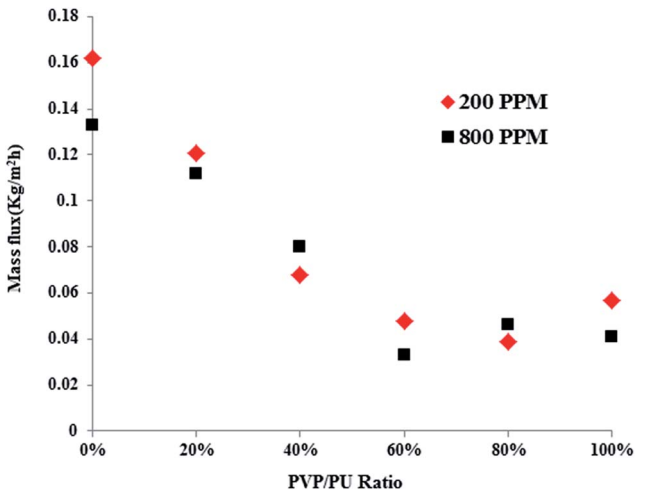

Fig. 8 Effect of sulfur content on the permeation flux. $T = 25$ °C.

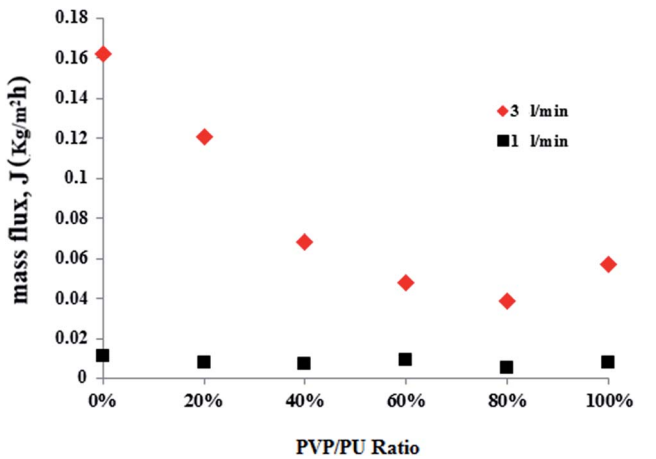

Fig. 9 Effect of feed flow rate on mass flux.

This journal is © The Royal Society of Chemistry 2015

Published on 27 October 2015. Downloaded by Indian Institute of Technology New Delhi on 19/11/2015 06:28:05.

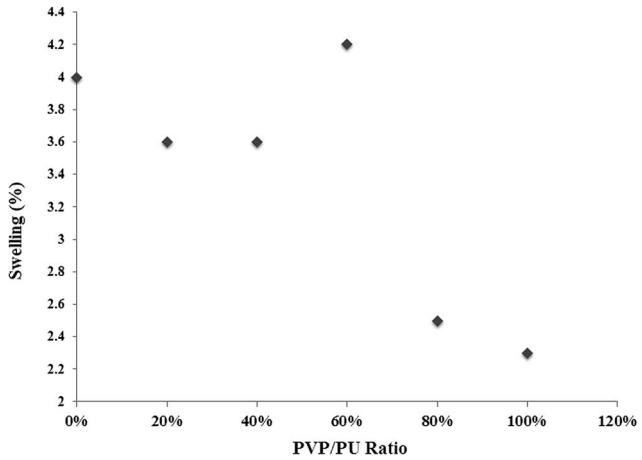

Fig. 10 Percentage of membrane swelling at different PVP/PU ratios.

3.3 Effect of PVP concentration on desulfurization

The effect of PVP concentration on the mass transfer flux and the enrichment factor of sulfur is shown in Fig. 6. PVP/PU membranes were prepared at PVP/PU ratios of 0–1. The amount of water in the feed solution was 100 ppm, which was half the sulfur content in the feed stream. Owing to the hydrophilic nature of PVP,[49–51] increasing the PVP content in the membrane increased the water flux dramatically compared with the sulfur flux. Consequently, the sulfur mass flux through the membrane decreased. In addition, adding PVP to membrane reduced the interaction between organic compounds and PVP. Thus, the permeation of the feed, which was mostly organic compounds, through the membrane decreased. However, the enrichment factor fluctuated between 1.11 and 1.57. The optimum PVP/PU ratio was 0.2. In addition, as the PVP concentration was increased from 0% to 20%, the enrichment factor increased from 1.111 to 1.57. This can be explained by the solubility parameters of typical sulfur species and PVP. The solubility parameters of PVP and sulfur species are 20.56 and 19–20, respectively. Therefore, more sulfur compounds penetrate the membrane because similar solubility parameters increase the affinity of sulfur species for the composite PVP/PU membrane.[52]

3.4 Effect of sulfur content in the feed

The effect of the sulfur content in the feed on the mass transfer flux and enrichment factor are shown in Fig. 7 and 8. The sulfur

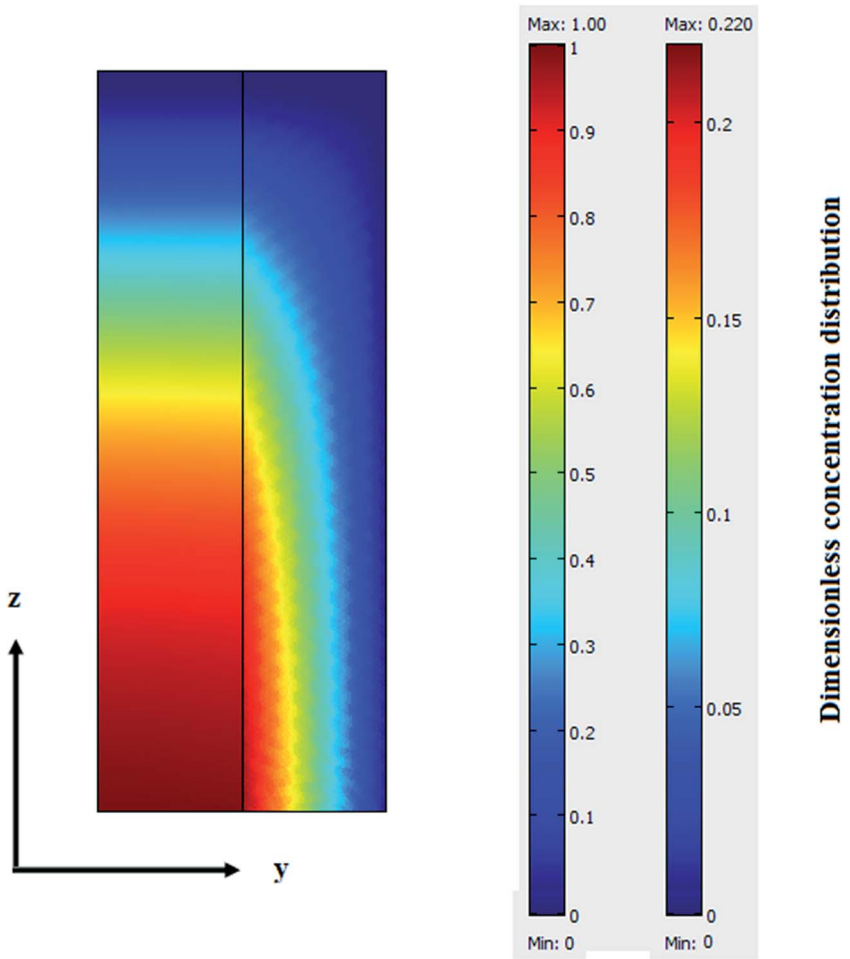

Fig. 11 Concentration distribution of sulfur in the feed and membrane compartments.

Published on 27 October 2015. Downloaded by Indian Institute of Technology New Delhi on 19/11/2015 06:28:05.

concentration in the feed solution increased from 220 to 800 ppm at a feed temperature of 298 K. The sulfur concentration has a considerable effect on the enrichment factor, especially at lower feed concentrations. Fig. 7 shows that an increase in sulfur content in the feed decreases the sulfur enrichment factor sharply. Hydrocarbon compounds do not diffuse readily into non-swollen membranes, whereas they do diffuse easily through swollen membranes. Therefore, the sorption selectivity for sulfur decreased with increasing sulfur content in the feed. Fig. 8 suggests that the swelling balance in the membrane and the saturated sulfur concentration on the surface of the membrane may have changed the flux factor slightly as the sulfur content of the feed increased.

3.5 Effect of feed flow rate

The mass transfer flux of sulfur increased with the increase in feed flow rate (Fig. 9), owing to the decrease in concentration polarization and temperature polarization. Generally, concentrations of sulfur compounds on membrane surfaces that contain more permeable components are lower than concentrations in bulk solution. Reducing the concentration polarization made the sulfur concentration near the membrane wall similar to the bulk concentration. The increase in sulfur concentration on the membrane surface with the feed rate increased the sorption of sulfur compounds and swelling in the membrane, increasing the mass transfer flux. The results indicated that operating the pervaporation system at high flow rate is desirable.

3.6 Percentage of membrane swelling at different PVP/PU ratios

The percentage of swelling at various PVP/PU ratios from 0 to 1 is shown in Fig. 10. During the swelling test, the membranes were weighed every 1 h for 5 h. The membranes were placed in the solvent for 72 h to ensure that they reached steady state conditions. The swelling decreased with increasing PVP content in the membrane. This result was attributed to the increase in the hydrophilicity of the membrane.

3.7 Modeling results

3.7.1 Concentration distribution of sulfur. The sulfur concentration distributions on the feed and membrane sides are shown in Fig. 11. The concentration is shown in dimensionless form. The feed solution containing sulfur and gasoline enters the pervaporation system where the sulfur has a maximum concentration (C_0). Sulfur is transferred from the bulk feed to the membrane wall because the concentration difference is the driving force on the feed side. Diffusion and convection are the sulfur transfer mechanisms on the feed side. The sulfur then diffuses through the dense membrane. Finally, sulfur is evaporated by the induced vacuum on the membrane–permeate interface. The sulfur concentration at the permeate–membrane interface is assumed to be negligible because of the low pressure induced by the vacuum pump.

4 Conclusions

Refinery naphtha feed desulfurization of gasoline can be accomplished by pervaporation with a PU/PVP membrane. The contact angle and surface tension results revealed that adding PVP to the PU membrane reduces the contact angle and surface tension, which confirms the hydrophilicity of the PVP/PU membranes. Permeation mass flux decreased with increasing sulfur content in the feed stream, whereas it increased with the feed temperature. The sulfur enrichment factor remained constant at first, and then decreased when the temperature increased. The permeation flux increased with increasing feed flow rate in the membrane module. The permeation flux did not change as the sulfur enrichment factor decreased as the feed sulfur content increased in the feed stream. Furthermore, a mathematical model was developed to simulate the separation of sulfur from sulfur/gasoline solution.

Nomenclature

A	Effective area of membrane (m^2)
C_s	Sulfur concentration (mol m^{-3})
$C_{s\text{-feed}}$	Feed sulfur concentration (mol m^{-3})
$C_{s\text{-membrane}}$	Membrane sulfur concentration (mol m^{-3})
C_0	Inlet sulfur concentration (mol m^{-3})
D	Diffusion coefficient (m^2 s^{-1})
F	Body force (N)
J	Total permeation flux (kg m^{-2} h^{-1})
L	Module length (m)
m	Partition coefficient of sulfur between feed and membrane (-)
p	Pressure (Pa)
R_E	Chemical reaction (mol m^{-3} s^{-1})
R	Gas constant (J mol^{-1} K^{-1})
t	Time (s)
V	Velocity vector (m s^{-1})
x	Axis coordinate (m)
y	Axis coordinate (m)

Abbreviations

PU	Polyurethane
PVP	Poly(vinyl chloride)
PV	Pervaporation
FEM	Finite element method

Greek symbols

ρ	Feed solution density (kg m^{-3})
μ	Feed solution viscosity (kg m^{-1} s^{-1})

This journal is © The Royal Society of Chemistry 2015

Published on 27 October 2015. Downloaded by Indian Institute of Technology New Delhi on 19/11/2015 06:28:05.

Subscripts

w	Water
m	Membrane
S	Sulfur

References

1 R. A. Amaral, A. C. Habert and C. P. Borges, *Mater. Lett.*, 2014, **137**, 468–470.
2 H. R. Mortaheb, F. Ghaemmaghami and B. Mokhtarani, *Chem. Eng. Res. Des.*, 2012, **90**, 409–432.
3 T. G. Kaufmann, A. Kaldor, G. F. Stuntz, M. C. Kerby and L. L. Ansell, *Catal. Today*, 2000, **62**, 77–90.
4 C. Song, *Catal. Today*, 2003, **86**, 211–263.
5 R. Qi, Y. Wang, J. Chen, J. Li and S. Zhu, *J. Membr. Sci.*, 2007, **295**, 114–120.
6 F. L. Plantenga and R. G. Leliveld, *Appl. Catal., A*, 2003, **248**, 1–7.
7 M. F. Ali, A. Al-Malki, B. El-Ali, G. Martinie and M. N. Siddiqui, *Fuel*, 2006, **85**, 1354–1363.
8 M. Rezakazemi, K. Shahidi and T. Mohammadi, *Int. J. Hydrogen Energy*, 2012, **37**, 17275–17284.
9 M. Rezakazemi, K. Shahidi and T. Mohammadi, *Int. J. Hydrogen Energy*, 2012, **37**, 14576–14589.
10 M. Rostamizadeh, M. Rezakazemi, K. Shahidi and T. Mohammadi, *Int. J. Hydrogen Energy*, 2013, **38**, 1128–1135.
11 L. S. White, R. F. Wormsbecher and M. Lesemann, *U.S. Pat.*, 0211706 A1, 2004.
12 E. Ito and J. A. R. van Veen, *Catal. Today*, 2006, **116**, 446–460.
13 J. Chen, J. Li, R. Qi, H. Ye and C. Chen, *J. Membr. Sci.*, 2008, **322**, 113–121.
14 B. Li, S. Yu, Z. Jiang, W. Liu, R. Cao and H. Wu, *J. Hazard. Mater.*, 2012, **211–212**, 296–303.
15 L. Lin, Y. Kong, K. Xie, F. Lu, R. Liu, L. Guo, S. Shao, J. Yang, D. Shi and Y. Zhang, *Sep. Purif. Technol.*, 2008, **61**, 293–300.
16 L. Lin, Y. Kong and Y. Zhang, *J. Membr. Sci.*, 2008, **325**, 438–445.
17 B. S. Minhas, M. R. Chuba and R. J. Saxton, *U.S. Pat.*, 0026321 A1, 2004.
18 I. G. Wenten, *Membr. Sci. Technol.*, 2002, **24**, 1009–1024.
19 L. Lin, G. Wang, H. Qu, J. Yang, Y. Wang, D. Shi and Y. Kong, *J. Membr. Sci.*, 2006, **280**, 651–658.
20 L. Lin, Y. Kong, J. Yang, D. Shi, K. Xie and Y. Zhang, *J. Membr. Sci.*, 2007, **298**, 1–13.
21 L. Lin, Y. Zhang and Y. Kong, *Fuel*, 2009, **88**, 1799–1809.
22 Y. K. Fu Wei Lu, H. Ling Lv, J. Ding and J. R. Yang, *Adv. Mater. Res.*, 2011, **150–151**, 317–320.
23 Z.-J. Yang, Z.-Q. Wang, J. Li and J.-X. Chen, *Sep. Purif. Technol.*, 2013, **109**, 48–54.
24 R. Qi, Y. Wang, J. Chen, J. Li and S. Zhu, *Sep. Purif. Technol.*, 2007, **57**, 170–175.
25 R. Cao, X. Zhang, H. Wu, J. Wang, X. Liu and Z. Jiang, *J. Hazard. Mater.*, 2011, **187**, 324–332.
26 M. Jain, D. Attarde and S. K. Gupta, *J. Membr. Sci.*, 2015, **490**, 328–345.
27 Z. Yang, W. Zhang, J. Li and J. Chen, *Sep. Purif. Technol.*, 2012, **93**, 15–24.
28 L. Lin, Y. Kong, G. Wang, H. Qu, J. Yang and D. Shi, *J. Membr. Sci.*, 2006, **285**, 144–151.
29 R. Xu, G. Liu, X. Dong and W. Jin, *Desalination*, 2010, **258**, 106–111.
30 Z. Yang, T. Wang, X. Zhan, J. Li and J. Chen, *Ind. Eng. Chem. Res.*, 2013, **52**, 13801–13809.
31 M. Ghadiri and S. N. Ashrafizadeh, *Chem. Eng. Technol.*, 2014, **37**, 597–604.
32 M. Rezakazemi, A. Ghafarinazari, S. Shirazian and A. Khoshsima, *Polym. Eng. Sci.*, 2013, **53**, 1272–1278.
33 S. Shirazian, A. Marjani and M. Rezakazemi, *Eng. Comput.*, 2012, **28**, 189–198.
34 M. Fasihi, S. Shirazian, A. Marjani and M. Rezakazemi, *Math. Comput. Model.*, 2012, **56**, 278–286.
35 R. B. Bird, W. E. Stewart and E. N. Lightfoot, *Transport Phenomena*, John Wiley & Sons, New York, 2nd edn, 2002.
36 M. Ghadiri, M. Parvini and M. G. Darehnaei, *Polym. Eng. Sci.*, 2014, **54**, 2222–2227.
37 K. Tahvildari, A. Zarabpour, M. Ghadiri and A. Hemmati, *Polym. Eng. Sci.*, 2014, **54**, 2553–2559.
38 F. Barati, M. Ghadiri, R. Ghasemi and H. M. Nobari, *Chem. Eng. Technol.*, 2014, **37**, 81–86.
39 M. Ghadiri, V. Abkhiz, M. Parvini and A. Marjani, *Chem. Eng. Technol.*, 2014, **37**, 543–550.
40 M. Ghadiri, S. Fakhri and S. Shirazian, *Polym. Eng. Sci.*, 2014, **54**, 660–666.
41 M. Ghadiri, M. Ghasemi Darehnaei, S. Sabbaghian and S. Shirazian, *Chem. Eng. Technol.*, 2013, **36**, 507–512.
42 M. Ghadiri, A. Marjani and S. Shirazian, *Int. J. Greenhouse Gas Control*, 2013, **13**, 1–8.
43 M. Ghadiri and S. Shirazian, *Chem. Eng. Process.*, 2013, **69**, 57–62.
44 S. A. Miramini, S. M. R. Razavi, M. Ghadiri, S. Z. Mahdavi and S. Moradi, *Chem. Eng. Process.*, 2013, **72**, 130–136.
45 F. Nosratinia, M. Ghadiri and H. Ghahremani, *J. Ind. Eng. Chem.*, 2014, **20**, 2958–2963.
46 J. Zhu, Y. Zhang, M. Tian and J. Liu, *ACS Sustainable Chem. Eng.*, 2015, **3**, 690–701.
47 A. Wolińska-Grabczyk, *J. Membr. Sci.*, 2006, **282**, 225–236.
48 V. S. Cunha, M. L. L. Paredes, C. P. Borges, A. C. Habert and R. Nobrega, *J. Membr. Sci.*, 2002, **206**, 277–290.
49 G. O. K. Loh, Y. T. F. Tan and K. K. Peh, *Powder Technol.*, 2014, **256**, 462–469.
50 E.-J. Kim, M.-K. Chun, J.-S. Jang, I.-H. Lee, K.-R. Lee and H.-K. Choi, *Eur. J. Pharm. Biopharm.*, 2006, **64**, 200–205.
51 M. Moneghini, A. Carcano, G. Zingone and B. Perissutti, *Int. J. Pharm.*, 1998, **175**, 177–183.
52 K. Liu, C.-J. Fang, Z.-Q. Li and M. Young, *J. Membr. Sci.*, 2014, **451**, 24–31.